Article

Kinetically Controlled Lifetimes in Redox-responsive Transient Supramolecular Hydrogels

Jonathan Wojciechowski, Adam D. Martin, and Pall Thordarson

J. Am. Chem. Soc., **Just Accepted Manuscript** • DOI: 10.1021/jacs.7b12198 • Publication Date (Web): 06 Feb 2018

Kinetically Controlled Lifetimes in Redox-responsive Transient Supramolecular Hydrogels

Jonathan P. Wojciechowski, Adam D. Martin, Pall Thordarson*

School of Chemistry, the Australian Centre for Nanomedicine and The ARC Centre of Excellence in Convergent Bio-Nano Science and Technology, the University of New South Wales, Sydney, NSW 2052, Australia

Temporal control, transient assemblies, programmable materials, hydrogels, supramolecular chemistry

ABSTRACT: It remains challenging to program soft materials to show dynamic, tunable time-dependent properties. In this work, we report a strategy to design transient supramolecular hydrogels based on kinetic control of competing reactions. Specifically, the pH triggered self-assembly of a redox-active supramolecular gelator, *N,N'*-dibenzoyl-L-cystine (DBC) in the presence of a reducing agent, which acts to disassemble the system. The lifetimes of the transient hydrogels can be tuned simply by pH or reducing agent concentration. We find through kinetic analysis that gel formation hinders the ability of the reducing agent and enables longer transient hydrogel lifetimes than would be predicted. The transient hydrogels undergo clean cycles, with no kinetically trapped aggregates observed. As a result, multiple transient hydrogel cycles are demonstrated and can be predicted. This work contributes to our understanding of designing transient assemblies with tunable temporal control.

Introduction

The self-assembly of low-molecular-weight-gelators (LMWGs) has proven to be an effective strategy to design highly functional materials based on chemically well-defined small molecules.[1–4] LMWGs have shown excellent potential in a wide variety of applications such as three-dimensional cell culture,[5] light harvesting,[6,7] logic gates,[8] and inhibiting cancer cells.[9,10] Whilst these materials show exceptional stimuli responsiveness, they lack the complexity of natural systems, which show dynamic properties in space and time.[11–13] Key to achieving spatiotemporal control in these systems is a firm understanding of the self-assembly process and the kinetics of gelation.[14] Exceptional spatial control has enabled self-sorting of multi-component LMWGs based on their pK_a values,[15] which enables hydrogel networks to be selectively removed[16] or asssembled.[17] In contrast, strategies to tune the time-dependent properties of these materials remain limited.

Conceptually, designing materials with temporal control is a balancing act between the activation and deactivation kinetics of the system.[12] Strategies to achieve autonomous temporal control include the use of chemically fuelled assemblies,[18–21] competing enzyme reactions,[22,23] delayed enzymatic pH cycles[24,25] and enzyme coupled programmed reactions within a polymer.[26] Of these systems, however, examples which do not utilise enzymes are less common. As such, there is a growing interest in the design of transient assemblies controlled by chemical reactions, and under relatively biologically relevant benign conditions.[20]

To address this, we envisioned the design of a transient hydrogel system based upon competing chemical reactions with orthogonal methods of activation and deactivation. We proposed using supramolecular gelators, as the rate of gelation can proceed rapidly (*i.e.,* within seconds) upon addition of a suitable trigger. In addition, we found reduction of the disulfide bond in *N,N'*-dibenzoyl-L-cystine (**DBC**), a well-known supramolecular gelator,[27] diminished its aggregation ability. Shown schematically in Figure 1, we designed a transient hydrogel based on the competitive self-assembly of **DBC** in the presence of a disulfide reducing agent, tris(2-carboxylethyl)phosphine (TCEP).

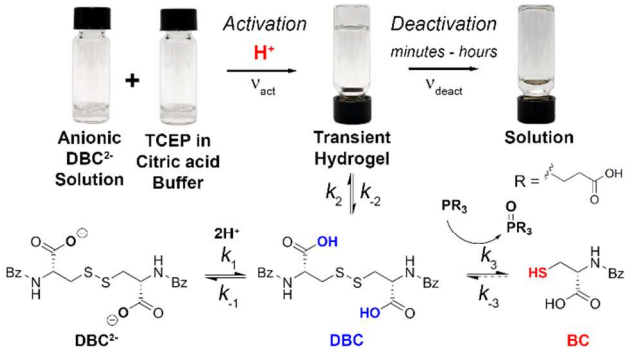

Figure 1. Schematic of the sol→gel→sol cycle of the transient hydrogels. Mixing anionic **DBC**$^{2-}$ with TCEP in citric acid buffer yields hydrogels, triggered from the pH dependent self-assembly of **DBC**. The hydrogel formed is transient because TCEP slowly reduces **DBC** to *N*-benzoyl-L-cystine (**BC**), resulting in dissolution of the hydrogel (sol→gel→sol). The lifetimes of the hydrogels can be chemically controlled by pH or initial TCEP concentration.

In this study, we show that we can create transient hydrogels with autonomous sol→gel→sol transitions based

on kinetic control of competing chemical reactions (Figure 1). This strategy can be used to tune the lifetimes of the transient hydrogels based on pH or the concentration of TCEP. We show through kinetic experiments an understanding of the mechanism of the sol→gel→sol cycle of the transient hydrogels. In addition, we show this system can achieve multiple transient hydrogel cycles.

Results and discussion

Transient hydrogel design

A conceptual framework for designing systems that exhibit autonomous time dependent properties is such that the rate of activation, ν_{act} is much greater than the rate of deactivation, ν_{deact}.[12,13] This allows the activated self-assembled structures to temporarily exist before they are deactivated by a competing reaction. Redox-active supramolecular gelators are ideal for this because they biologically relevant and impart orthogonal stimuli responsiveness. For example the reduction of disulphides[28,29] and oxidation of thiols[30] have both been used to trigger gelation. Moreover, the redox activity of disulphides is commonly utilised to cross-link polymeric hydrogels.[31] Due to the orthogonal activation and deactivation kinetics, we reasoned that we could control the kinetics of the competing reactions to tune the lifetimes of the self-assembled LMWG hydrogels.

The kinetics of the transient **DBC** hydrogels can be defined by the equilibrium constants shown in Figure 1. Gelation is activated when anionic **DBC**$^{2-}$ is protonated to **DBC** (Figure 1). Charge screening of the carboxylate initiates rapid self-assembly of **DBC** into a supramolecular hydrogel driven by non-covalent interactions, namely hydrophobic, π-π and van der Waal interactions.[27] The self-assembly of **DBC** competes in the presence of a reducing agent (TCEP) that reduces the disulfide bond, to give *N*-benzoyl-L-cysteine **BC**, resulting in dissolution of the hydrogel (Figure 1).

A phosphine based reducing agent (TCEP) was chosen due to the acidic pH used to trigger the hydrogels (pH 3.00 and below). Other common water-soluble reducing agents such as dithiothreitol (DTT), 2-mercaptoethanol and dithiolbutylamine (DTBA) require higher pH (5.00 and above) since reduction occurs through thiol-disulfide interchange by the reducing agent thiolate, with typical pK_a values = 8.2 – 9.6.[32] In contrast, TCEP proceeds rapidly at low pH due to the pH independence of the phosphine nucleophile.[33]

Protonation of **DBC** (k_1) is not rate determining, hence the lifetimes of the transient hydrogels can be controlled by understanding the factors which affect the rate of gelation (k_2) and the rate of reduction (k_3). In addition, the backwards oxidation reaction (k_{-3}) is negligible since the systems operates at acidic pH (pH < 3.00). Based on the unique dynamics of this system, we aimed to fully investigate the kinetics of the transient hydrogels as a function of pH and initial concentration of TCEP, which allows the hydrogel lifetimes to be tuned.

pH dependence on transient hydrogel lifetimes

In aqueous solvents, protonation of **DBC**$^{2-}$ to **DBC** (k_1) initiates the self-assembly of **DBC** into a hydrogel (k_2). The self-assembly of **DBC** occurs at pH values below the pK_a, and is a well-known mechanism for supramolecular gelators.[15] To our knowledge, the pK_a value for **DBC** has not been reported, only estimated,[19] hence we determined the pK_a of **DBC** by pH titration and found it to be 3.58 (Figure S1). A pH switch method was used to trigger gelation by mixing 1:1 (v/v) anionic **DBC**$^{2-}$ with 100 mM citric acid/trisodium citrate buffer. To make transient hydrogels, a solution of TCEP in 100 mM citric acid/trisodium citrate buffer was used. This method of pH switch was chosen over commonly used lactone hydrolysis[34] due to faster gelation rates of **DBC**, whilst still yielding consistent hydrogels unlike HCl-based methods.

The rate of gelation of **DBC** (k_2) is dependent on pH, with a pH closer to the pK_a resulting in a slower gelation rate (Table S1). As a result of the competing reactions in the transient hydrogels from the introduction of TCEP, a boundary condition pH exists that is dictated by the rate of gelation. Gelation must be significantly faster than the reduction rate of TCEP to form transient hydrogels. To determine this pH value, pH dependent time-resolved rheology was conducted at pH values below the pK_a on 5 mM **DBC** hydrogels with an excess of TCEP = 10 mM (Figure 2a). The ratio of citric acid:trisodium citrate was altered to change the pH of the hydrogels (Figure S2). To measure the rheological properties of these transient hydrogels, a constant frequency of 1 Hz and strain of 0.1% was used, which shows no frequency dependent behavior and lies within the linear viscoelastic region for these hydrogels (Figure S3). The lifetime of the transient hydrogels is defined by the time they are no longer self-supporting by the vial inversion test (G' ≈ 50 Pa).

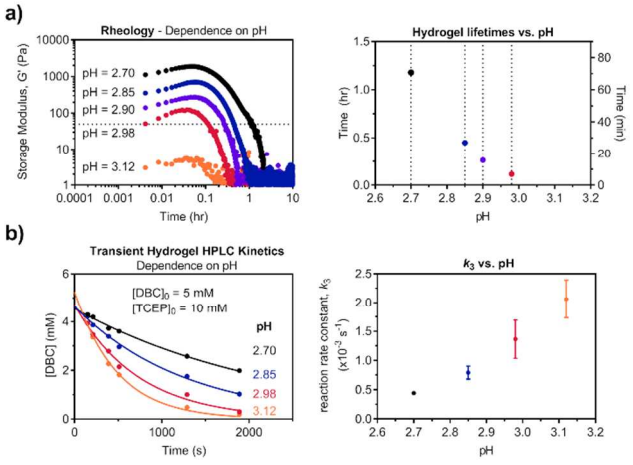

Figure 2. a) pH dependent rheology shows an increase in hydrogel lifetimes and storage modulus (G') with a decrease in pH. b) HPLC kinetics of **DBC** reduction in the hydrogel shows the rate of reduction of **DBC** is slower as the pH decreases. For both experiments: [**DBC**]$_0$ = 5 mM, [TCEP]$_0$ = 10 mM. Error bars on uncertainty are the 95% confidence interval (*nlparci* function in *matlab*).

The pH dependent rheology of the transient hydrogels shows a boundary condition pH lower than the pK_a of **DBC**. Hydrogels triggered at pH = 3.12 only form viscous solutions, as shown by a small increase in G' below 5 Pa, but are not self-supporting as demonstrated by the vial inver-

sion test. In contrast, transient hydrogels are formed at pH values of 2.98 and below, which indicates the rate of gelation is faster than the rate of reduction of **DBC**. Unexpectedly, the lifetimes of the transient hydrogels increase as the pH decreases. Transient hydrogels formed at pH = 2.98 have lifetimes of 7 minutes compared with hydrogels formed at pH = 2.70 which have significantly longer lifetimes of 70 minutes. The reduction mechanism of TCEP is pH independent,[33] and hence the increase in lifetimes must be attributed to the formation of hydrogels. This indicates once **DBC** forms supramolecular assemblies, the rate of reduction by TCEP is reduced. Indeed, the formation of supramolecular assemblies have shown to reduce reaction kinetics in a related dissipative supramolecular hydrogel system.[20]

We sought to measure the kinetics of **DBC** reduction (k_3 – we assume $k_{-3} = 0$) in a hydrogel and developed a HPLC method to achieve this (See SI for details). In brief, transient hydrogels are formed, dissolved in 14-fold volume-excess of methanol at various kinetic time points and injected into the HPLC. The concentrations of DBC were determined using a HPLC calibration curve of the peak areas (Figure S4). The concentration of **DBC** with respect to time were fit to pseudo-first order kinetic equations to determine the reaction rate constant, k. The HPLC kinetic data on the transient hydrogels shown in Figure 2b shows slower reduction kinetics of **DBC** as the pH is decreased and agrees with the rheology data. The reaction rate constant at pH 3.12, where a gel is not formed, is 2.06 ± 0.12 x 10^{-3} s^{-1} and is almost five times larger than the reaction rate constant at pH 2.70, k = 0.443 ± 0.016 x 10^{-3} s^{-1}, which shows the longest hydrogel lifetimes.

Taken together, the pH dependent rheology and HPLC kinetics of the hydrogels show that upon assembly of **DBC** into a transient hydrogel, the kinetics of **DBC** reduction is reduced, and therefore the lifetimes of the hydrogels increase. These results indicate the mechanism of transient hydrogel reduction likely occurs through dissociation of **DBC** from the transient hydrogel, which is then rapidly reduced by TCEP to **BC**. Once **DBC** is reduced, it is unable to exchange with the supramolecular fibres and hence the hydrogel is slowly dissolved. The dissociation of gelator monomers from self-assembled fibres is a well-known mechanism and has been observed in related one-dimensional fibres.[35]

This is an interesting property, since control of the dissociation constant of the hydrogel (k_{-2}) affects the lifetime of the supramolecular assemblies. In summary, there is a clear pH dependence on the lifetimes of the transient hydrogels. Above pH ≈ 3.00, transient hydrogels will not form because the rate of gelation does not outcompete the rate of reduction. Below pH ≈ 3.00, transient hydrogels can be formed due to a higher rate of gelation. These results show the lifetimes of the transient hydrogels can be tuned by pH.

The effect of TCEP on transient hydrogel lifetimes

Next, we sought to investigate the rate of reduction in the transient hydrogels with increasing concentrations of TCEP. We expected higher concentrations of TCEP would increase the rate of **DBC** reduction and allow another parameter to control the transient hydrogel lifetimes. Based on the pH dependent results, a 100 mM 85/15 (v/v) citric acid/trisodium citrate buffer was chosen due to sufficient rates of gelation, yet also allow for sufficient mixing times (*ca.*, 20 s). The final pH of the transient hydrogels was in the range of pH = 2.70 - 3.00.

We performed time-resolved rheology on 5 mM **DBC** transient hydrogels with varying concentrations of TCEP (5-20 mM). As shown in Figure 3a, the storage modulus (G') of the **DBC** hydrogels decrease faster in the presence of higher concentrations of TCEP, and show reduced hydrogel lifetimes. All hydrogels reach a maximum storage modulus of 600-700 Pa, before decreasing with time. As expected, higher equivalents of TCEP results in a shorter hydrogel lifetime, due to the faster rate of reduction on **DBC**. The lifetimes of the transient hydrogels are as short as 14 minutes for 5 mM **DBC** with 20 mM TCEP (4 equiv.) or as long as 82 minutes when 5 mM TCEP (1 equiv.) is used, showing a clear dependence on initial concentration of TCEP. Interestingly, the lifetimes of the transient hydrogels with $[TCEP]_0$ = 5 mM are significantly longer than the higher initial concentrations of TCEP, which show an almost linear relationship. To understand the process behind this increase in the hydrogel lifetimes, HPLC kinetics were performed on the hydrogels to investigate the dependence on $[TCEP]_0$. A constant concentration of **DBC** = 5 mM was used, with the concentration of TCEP varied between 5-20 mM.

Figure 3b shows the concentration of **DBC** in a hydrogel at various time points with increasing $[TCEP]_0$. The HPLC data was fit to a pseudo-first order kinetic equation with respect to **DBC** degradation, which is found for TCEP in solution.[33]

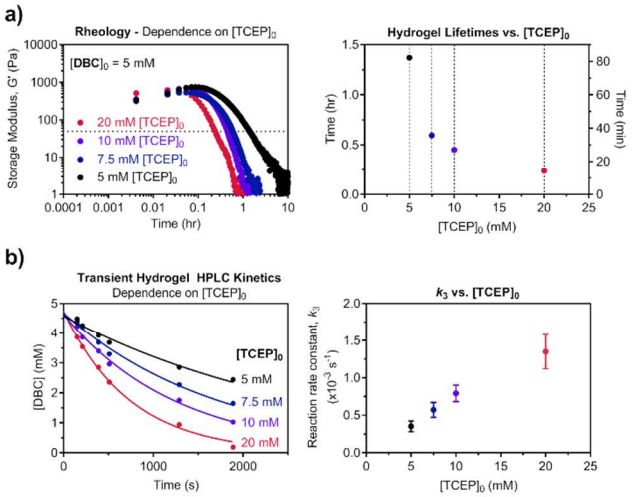

Figure 3. a) Time-resolved rheology of 5 mM **DBC** hydrogels shows a decrease in the hydrogel lifetimes with increasing concentrations of TCEP. b) Kinetic analysis of the rate of reduction of 5 mM **DBC** transient hydrogels by TCEP fits to a pseudo-first order kinetic equation. Error bars on uncertainty are the 95% confidence interval (*nlparci* function in *matlab*).

The plot of k_3 versus initial concentration of TCEP shows a linear relationship, which is not seen in the hydrogel lifetimes by rheology. Based on the previous results showing the pH dependence of k_3, it is known that formation of the hydrogel hinders reduction of **DBC**. Therefore, the reduc-

tion of **DBC** to **BC** likely occurs when it is dissociated from the hydrogel. In the case of the pH dependent results, an excess of TCEP (2 equiv.) was used to study these kinetics, and it can be assumed once **DBC** is dissociated, it would likely be reduced to **BC**. In the case of $[TCEP]_0$ = 5 mM, the ratio is stoichiometric, and it is possible the rate of **DBC** reduction is slower than association of **DBC** to the hydrogel. This suggests that **DBC** is not being constantly reduced when dissociated, which would increase the lifetimes of the hydrogel. This is further exemplified when the pH of the hydrogel is decreased, giving hydrogel lifetimes of 6.7 hours in the case of a 95/5 citric acid/trisodium citrate buffer (Figure S5). This result further supports the hypothesis that once **DBC** self-assembles into a hydrogel, the rate of reduction by TCEP is limited by the dissociation of **DBC**. As a result, the dissociation constant of the hydrogel (k_{-2}) is potentially rate limiting the reduction of **DBC** to **BC**.

Morphology and secondary structure changes in the transient hydrogel cycle

Clearly, the lifetime of the hydrogels can be tuned by changing the pH or initial concentration of TCEP. We were interested to visualize the self-assembled structures which form in the cycle, since in some cases kinetically trapped products are formed upon assembly and disassembly.[14,16,22] These kinetically trapped products are undesirable, reducing the efficiency of multiple transient cycles. We firstly investigated the nanostructures using atomic force microscopy of the pre-gel solutions (**DBC**$^{2-}$), hydrogels (**DBC**) and reduced gel solutions (**BC**) (Figure S6).

Initially, no structures are observed in the anionic **DBC**$^{2-}$ solution, suggesting monomeric solvation of the solution. Upon acidification of this solution, fibrous networks are observed by AFM for the **DBC** hydrogels, which is consistent with previously reported network structures for these hydrogels.[27] Upon reduction to **BC**, these fibrous structures are no longer detected by AFM. In addition, small aggregate structures are also not observed which is assumed to be the result of high solubility of the reduced **BC**, and hence it does not form any aggregates.

The monomeric solvation of **DBC**$^{2-}$ and **BC** is supported by ^{1}H NMR and viscosity measurements which shows sharp, resolved peaks in ^{1}H NMR (Figure S7) and that viscosity is independent of shear rate (Figure S8). Combined, these results show that the **DBC** hydrogels do not form kinetically trapped aggregates upon reduction, demonstrating the clean assembly and disassembly of the transient hydrogels.

To gain insights into the morphology changes during transient hydrogel disassembly we conducted a time-resolved AFM study on a 5 mM **DBC** transient hydrogel with 5 mM TCEP (Figure 4a-d). Initially, 10 and 30 minutes after hydrogel formation (Figure 4a-b), the transient hydrogels show a thick, fibrous network similar to the **DBC** hydrogels in Figure S6b. One hour after hydrogel formation (Figure 4c), the fibrous network is noticeably less dense compared with the 10 and 30 minutes images. After two hours (Figure 4d), only short fibers of randomly distributed lengths are observed. This agrees with the rheology data (Figure 3a) which shows the hydrogels display some viscoelastic properties at two hours, however, do not form self-supporting hydrogels. Thus, the time-resolved AFM measurements suggests the transient hydrogel network initially starts as a population of large, cross-linked fibers which over time lessen in both fiber size and fiber length.

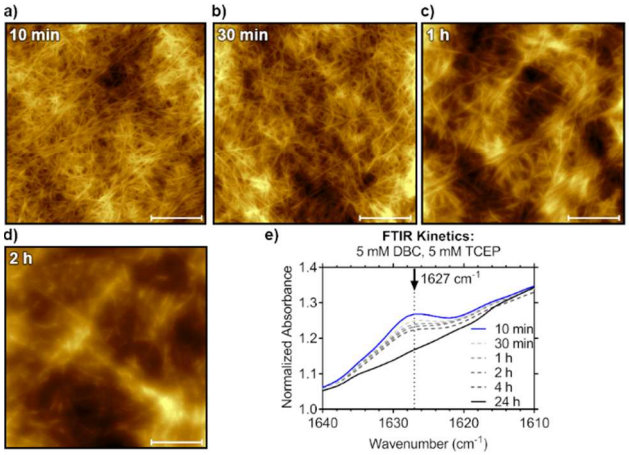

Figure 4. a-d) Time-resolved atomic force microscopy of a 5 mM **DBC** transient hydrogel with 5 mM TCEP; a) 10 min, b) 30 min, c) 1 h (60 min) and d) 2 h (120 min). e) Time-resolved FTIR on a 5 mM **DBC** transient hydrogel with 5 mM TCEP in D_2O shows a decrease in the amide C=O stretch at 1627 cm^{-1} with respect to time. Scale bars represent 1 μm.

As AFM had revealed a change in the density and length of the fibrous network for the transient hydrogels over time, we then used FTIR to probe whether a change in secondary structure was also observed. The **DBC** hydrogels display a peak at 1627 cm^{-1}, which represents the C=O stretching vibrations of the amide bond (Figure S9). This stretching frequency is not observed in the anionic **DBC**$^{2-}$ solution, **BC** solution or TCEP solution, and hence can be used to monitor the disassembly of the transient hydrogels (Figure S9).

To follow the kinetics of transient hydrogel disassembly, 5 mM **DBC** hydrogels with 5 mM TCEP were used (Figure 4e). Initially, the transient hydrogels show the characteristic C=O stretching frequency at 1627 cm^{-1} (10 minutes) found in the **DBC** hydrogels. This stretching frequency decays over four hours as the assemblies are reduced by TCEP. No increase in other peaks in the Amide I region (1700 – 1600 cm^{-1}) are observed. This result suggests the transient hydrogel assemblies do not undergo any changes to their secondary structure upon dissolution.

Multiple pre-programmed transient hydrogel cycles.

A significant challenge in transient assemblies which show temporal control is the ability to complete multiple reaction cycles without degradation of the system components.[23,26,36] Encouraged by the clean assembly and disassembly of the hydrogels, we sought to benchmark this approach to achieve multiple transient hydrogel cycles (*i.e.*, sol→gel→sol after addition of a trigger). Multiple cycles of transient assemblies are particularly interesting because they may be used in continuous stirred tank reactors or microfluidics to achieve out-of-equilibrium steady

states.[37,38] In addition, they could be applied in soft robotics or used in microfluidics as temporary fluid guides.

To achieve multiple transient hydrogel cycles, we used an excess initial concentration of TCEP (Figure 5a). TCEP reacts stoichiometrically with **DBC**, hence we can preprogram the number of transient hydrogel cycles. Addition of **DBC**$^{2-}$ to the solution with TCEP causes formation of a transient hydrogel which is then autonomously converted over time to a solution (one cycle). Consequent addition of **DBC**$^{2-}$ to this solution enables another transient hydrogel cycle. The transient cycles can be repeated as long as the concentration of TCEP is sufficient to reduce the **DBC**$^{2-}$ added. We used UV-vis scattering at 350 nm to monitor the transient cycles since only the **DBC** hydrogels absorb at this wavelength (Figure S10). A typical scattering profile of the transient hydrogel cycle is shown in Figure 5b.

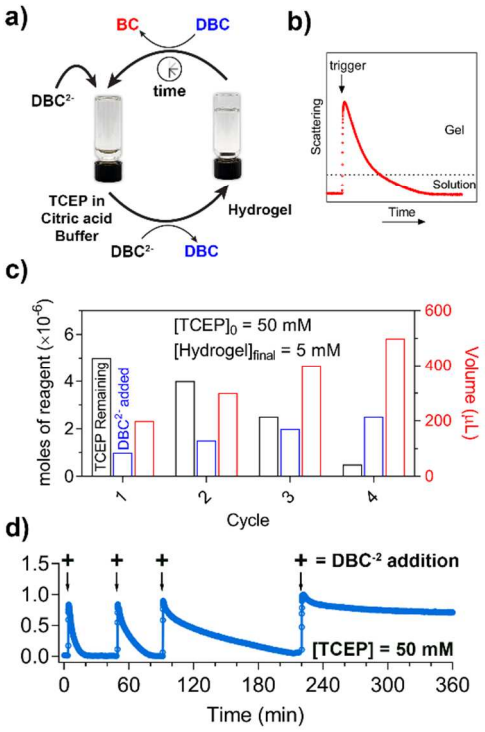

Figure 5. a) Schematic of the transient hydrogel cycles. The number of cycles can be programmed based on the starting concentration of TCEP. b) Typical time-resolved UV-vis scattering of the transient hydrogel cycle. c) Amount of TCEP remaining, **DBC**$^{2-}$ added and volume change after each cycle for $[TCEP]_0$ = 50 mM. d) UV-vis scattering showing three transient hydrogel cycles with a starting concentration of TCEP = 50 mM.

Initially, the solution of TCEP exhibits no scattering at 350 nm. Transient hydrogels are triggered upon the addition of **DBC**$^{2-}$, resulting in a rapid increase in the scattering which can be attributed to the formation of a hydrogel. The scattering then slowly decreases over time as **DBC** is reduced to **BC**, which does not absorb at 350 nm. On each cycle, the transient hydrogel concentration is always 5 mM. Due to the volume increases on each cycle, the concentration of **DBC**$^{2-}$ added increases on each cycle to maintain a hydrogel concentration = 5 mM and is shown in Figure 5c. Based on stoichiometry, an initial concentration of 50 mM TCEP has the capacity for three, 5 mM **DBC** transient hydrogel cycles.

Three transient hydrogel cycles can be seen in Figure 5d, monitored using UV-vis. The increase in scattering upon addition of **DBC**$^{2-}$ is due to transient hydrogel formation (Figure S11) The lifetimes of the hydrogels increase as TCEP is consumed, since higher equivalents of TCEP result in faster dissolution of the hydrogel which is shown by HPLC and rheology data. However, on the fourth cycle, there is not enough TCEP to reduce **DBC** and deactivate the hydrogel, hence the hydrogels do not dissolute. There is a small decrease in scattering as the remaining TCEP is consumed. The resulting hydrogel after the fourth cycle is kinetically stable, and remains self-supporting after 24 hours (Figure S11).

Conclusions

We have outlined a general approach to enable transient lifetimes in redox-active materials based on orthogonal reaction kinetics. In this work, we show competing kinetics of supramolecular gelation (activation) and disulfide reduction (deactivation) can be kinetically controlled to create transient hydrogels with show autonomous temporal control (*i.e.,* gel-sol reversibility without input). We study the mechanism of this system using rheology and HPLC and show the deactivation of the transient assemblies occurs through a dissociative pathway. Moreover, this study highlights the delicate balance between solubility and self-assembly. We show this approach can be used to achieve multiple transient hydrogel cycles, which can be predicted based on the concentrations of starting materials.

The insights gained from the kinetic analysis on this approach contributes to our understanding of spatiotemporal control in self-assembled structures. The general concept of competing chemical reactions outlined in this work is applicable not only to redox-active systems, but also stimuli responsive systems. We envision this concept will contribute to the strategies used in the next generation of spatiotemporal hydrogel material[39] and could potentially be used to create out-of-equilibrium systems using microfluidics or continuously stirred tank reactors.[37]

ASSOCIATED CONTENT

Supporting Information

Experimental procedures, details of kinetic analysis, HPLC method for transient hydrogels, pH titration, rheological characterization, NMR characterization, AFM images, FTIR spectra, viscosity and UV-Vis characterization are available free of charge on the ACS Publications website as a PDF.

AUTHOR INFORMATION

Corresponding Author

*p.thordarson@unsw.edu.au

Notes

The authors declare no competing financial interests.

ACKNOWLEDGMENT

We would like to thank the Mark Wainwright Analytical Centre (UNSW) for access to instruments. We acknowledge the Australian Research Council for an ARC Centre of Excellence grant (CE140100036) to P.T and National Health and Medical Research Council for a Dementia Development Research Fellowship (APP1106751) to ADM. We would also like to thank the Australian Government for an APA to J.P.W.

REFERENCES

(1) Draper, E. R.; Adams, D. J. *Chem* **2017**, *3*, 390–410.
(2) Fleming, S.; Ulijn, R. V. *Chem. Soc. Rev.* **2014**, *43*, 8150–8177.
(3) Du, X.; Zhou, J.; Xu, B. *Chem. Asian J.* **2014**, *9*, 1446–1472.
(4) Tao, K.; Levin, A.; Adler-Abramovich, L.; Gazit, E. *Chem. Soc. Rev.* **2016**, *45*, 3935–3953.
(5) Alakpa, E. V.; Jayawarna, V.; Lampel, A.; Burgess, K. V.; West, C. C.; Bakker, S. C. J.; Roy, S.; Javid, N.; Fleming, S.; Lamprou, D. A.; Yang, J.; Miller, A.; Urquhart, A. J.; Frederix, P. W. J. M.; Hunt, N. T.; Péault, B.; Ulijn, R. V.; Dalby, M. J. *Chem* **2016**, *1*, 298–319.
(6) Weingarten, A. S.; Kazantsev, R. V.; Palmer, L. C.; McClendon, M.; Koltonow, A. R.; Samuel, A. P. S.; Kiebala, D. J.; Wasielewski, M. R.; Stupp, S. I. *Nat. Chem.* **2014**, *6*, 1–30.
(7) Hestand, N. J.; Kazantsev, R. V.; Weingarten, A. S.; Palmer, L. C.; Stupp, S. I.; Spano, F. C. *J. Am. Chem. Soc.* **2016**, *138*, 11762–11774.
(8) Ikeda, M.; Tanida, T.; Yoshii, T.; Kurotani, K.; Onogi, S.; Urayama, K.; Hamachi, I. *Nat. Chem.* **2014**, *6*, 511–518.
(9) Feng, Z.; Wang, H.; Zhou, R.; Li, J.; Xu, B. *J. Am. Chem. Soc.* **2017**, *139*, 3950–3953.
(10) Feng, Z.; Zhang, T.; Wang, H.; Xu, B. *Chem. Soc. Rev.* **2017**, *46*, 6470–6479.
(11) Whitesides, G. M.; Grzybowski, B. A. *Science* **2002**, *295*, 2418–2421.
(12) Heinen, L.; Walther, A. *Soft Matter* **2015**, *11*, 7857–7866.
(13) Merindol, R.; Walther, A. *Chem. Soc. Rev.* **2017**, *46*, 5588–5619.
(14) Raeburn, J.; Zamith Cardoso, A.; Adams, D. J. *Chem. Soc. Rev.* **2013**, *42*, 5143–5156.
(15) Morris, K. L.; Chen, L.; Raeburn, J.; Sellick, O. R.; Cotanda, P.; Paul, A.; Griffiths, P. C.; King, S. M.; O'Reilly, R. K.; Serpell, L. C.; Adams, D. J. *Nat. Commun.* **2013**, *4*, 1480.
(16) Draper, E. R.; Eden, E. G. B.; McDonald, T. O.; Adams, D. J. *Nat. Chem.* **2015**, *7*, 848–852.
(17) Cornwell, D. J.; Daubney, O. J.; Smith, D. K. *J. Am. Chem. Soc.* **2015**, *137*, 15486–15492.
(18) Boekhoven, J.; Brizard, A. M.; Kowlgi, K. N. K.; Koper, G. J. M.; Eelkema, R.; van Esch, J. H. *Angew. Chem. Int. Ed.* **2010**, *49*, 4825–4828.
(19) Boekhoven, J.; Hendriksen, W. E.; Koper, G. J. M.; Eelkema, R.; van Esch, J. H. *Science* **2015**, *349*, 1075–1079.
(20) Tena-Solsona, M.; Rieß, B.; Grötsch, R. K.; Löhrer, F. C.; Wanzke, C.; Käsdorf, B.; Bausch, A. R.; Müller-Buschbaum, P.; Lieleg, O.; Boekhoven, J. *Nat. Commun.* **2017**, *8*, 15895.
(21) Spitzer, D.; Rodrigues, L. L.; Straßburger, D.; Mezger, M.; Besenius, P. *Angew. Chem. Int. Ed.* **2017**, *56*, 15461–15465.
(22) Pappas, C. G.; Sasselli, I. R.; Ulijn, R. V. *Angew. Chem. Int. Ed.* **2015**, *54*, 8119–8123.
(23) Sahoo, J. K.; Pappas, C. G.; Sasselli, I. R.; Abul-Haija, Y. M.; Ulijn, R. V. *Angew. Chem. Int. Ed.* **2017**, *56*, 6828–6832.
(24) Heuser, T.; Steppert, A.-K.; Lopez, C. M.; Zhu, B.; Walther, A.; Molano Lopez, C.; Zhu, B.; Walther, A. *Nano Lett.* **2015**, *15*, 2213–2219.
(25) Heinen, L.; Heuser, T.; Steinschulte, A.; Walther, A. *Nano Lett.* **2017**, *17*, 4989–4995.
(26) Postma, S. G. J.; Vialshin, I. N.; Gerritsen, C. Y.; Bao, M.; Huck, W. T. S. *Angew. Chem. Int. Ed.* **2017**, *56*, 1794–1798.
(27) Menger, F. M.; Caran, K. L. *J. Am. Chem. Soc.* **2000**, *122*, 11679–11691.
(28) Bowerman, C. J.; Nilsson, B. L. *J. Am. Chem. Soc.* **2010**, *132*, 9526–9527.
(29) Wang, H.; Yang, Z. *Nanoscale* **2012**, *4*, 5259.
(30) Chen, J.; Wu, W.; McNeil, A. J. *Chem. Commun.* **2012**, *48*, 7310–7312.
(31) Gyarmati, B.; Némethy, Á.; Szilágyi, A. *Eur. Polym. J.* **2013**, *49*, 1268–1286.
(32) Lukesh, J. C.; Palte, M. J.; Raines, R. T. *J. Am. Chem. Soc.* **2012**, *134*, 4057–4059.
(33) Burns, J. A.; Butler, J. C.; Moran, J.; Whitesides, G. M. *J. Org. Chem.* **1991**, *56*, 2648–2650.
(34) Adams, D. J.; Butler, M. F.; Frith, W. J.; Kirkland, M.; Mullen, L.; Sanderson, P. *Soft Matter* **2009**, *5*, 1856.
(35) Albertazzi, L.; van der Zwaag, D.; Leenders, C. M. A.; Fitzner, R.; van der Hofstad, R. W.; Meijer, E. W. *Science* **2014**, *344*, 491–495.
(36) Pappas, C. G.; Sasselli, I. R.; Ulijn, R. V. *Angew. Chem. Int. Ed.* **2015**, *54*, 8119–8123.
(37) Semenov, S. N.; Kraft, L. J.; Ainla, A.; Zhao, M.; Baghbanzadeh, M.; Campbell, V. E.; Kang, K.; Fox, J. M.; Whitesides, G. M. *Nature* **2016**, *537*, 656–660.
(38) Cvrtila, I.; Fanlo-Virgós, H.; Schaeffer, G.; Monreal Santiago, G.; Otto, S. *J. Am. Chem. Soc.* **2017**, *139*, 12459–12465.
(39) Brown, T. E.; Anseth, K. S. *Chem. Soc. Rev.* **2017**, *46*, 6532–6552.

Authors are required to submit a graphic entry for the Table of Contents (TOC) that, in conjunction with the manuscript title, should give the reader a representative idea of one of the following: A key structure, reaction, equation, concept, or theorem, etc., that is discussed in the manuscript. Consult the journal's Instructions for Authors for TOC graphic specifications.

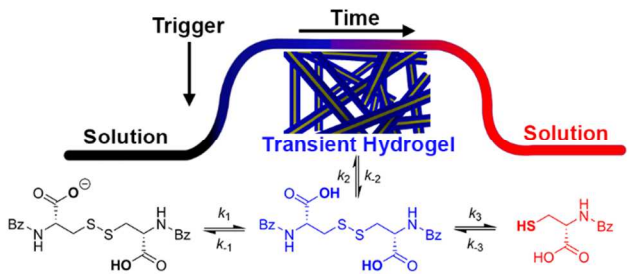

Insert Table of Contents artwork here

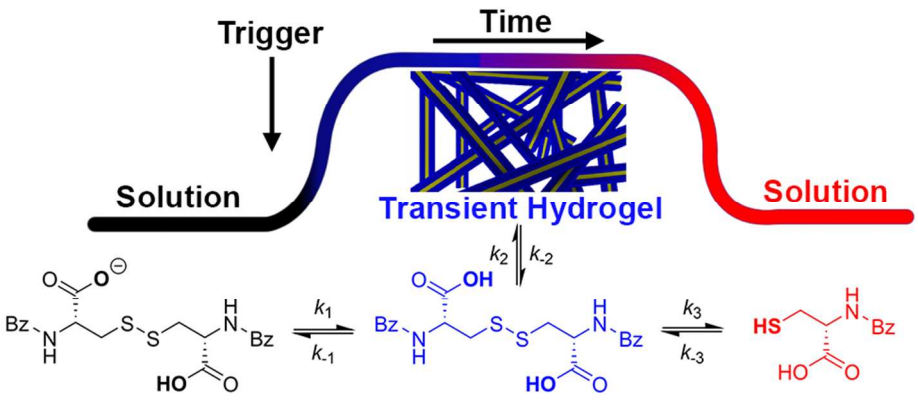

TOC Graphic

90x34mm (300 x 300 DPI)

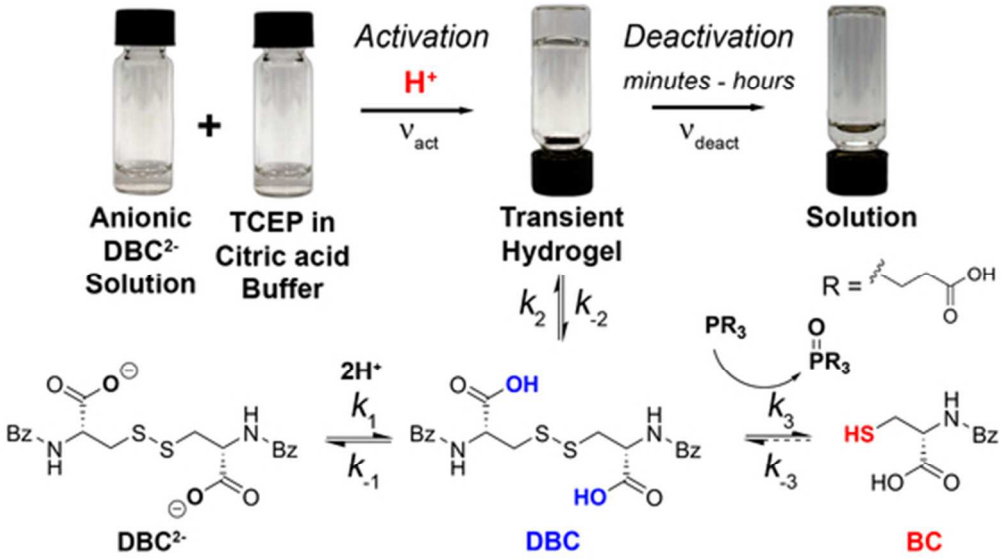

Figure 1. Schematic of the sol→gel→sol cycle of the transient hydrogels. Mixing anionic DBC^{2-} with TCEP in citric acid bufer yields hydrogels, triggered from the pH dependent self-assembly of **DBC**. The hydrogel formed is transient because TCEP slowly reduces DBC to N-benzoyl-L-cystine (**BC**), resulting in dissolution of the hydrogel (sol→gel→sol). The life-times of the hydrogels can be chemically controlled by pH or initial TCEP concentration.

46x26mm (300 x 300 DPI)

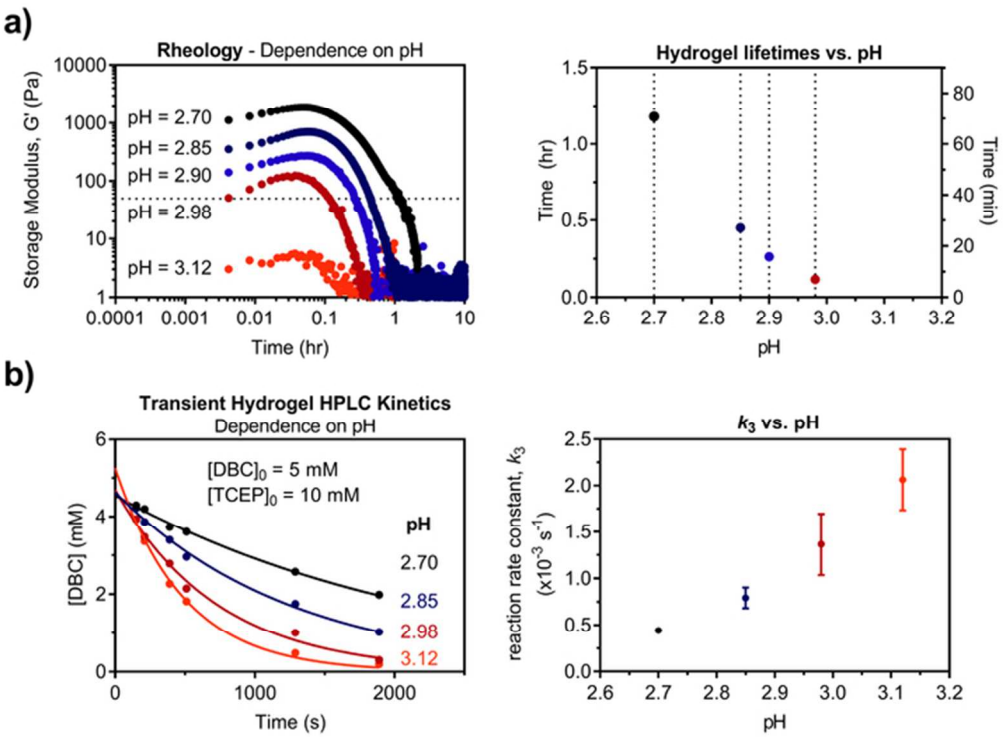

Figure 2. a) pH dependent rheology shows an increase in hydrogel lifetimes and storage modulus (G') with a decrease in pH. b) HPLC kinetics of **DBC** reduction in the hydrogel shows the rate of reduction of **DBC** is slower as the pH decreases. For both experiments: [**DBC**]$_0$ = 5 mM, [TCEP]$_0$ = 10 mM. Error bars on uncertainty are the 95% confidence interval (*nlparci* function in *matlab*).

60x44mm (300 x 300 DPI)

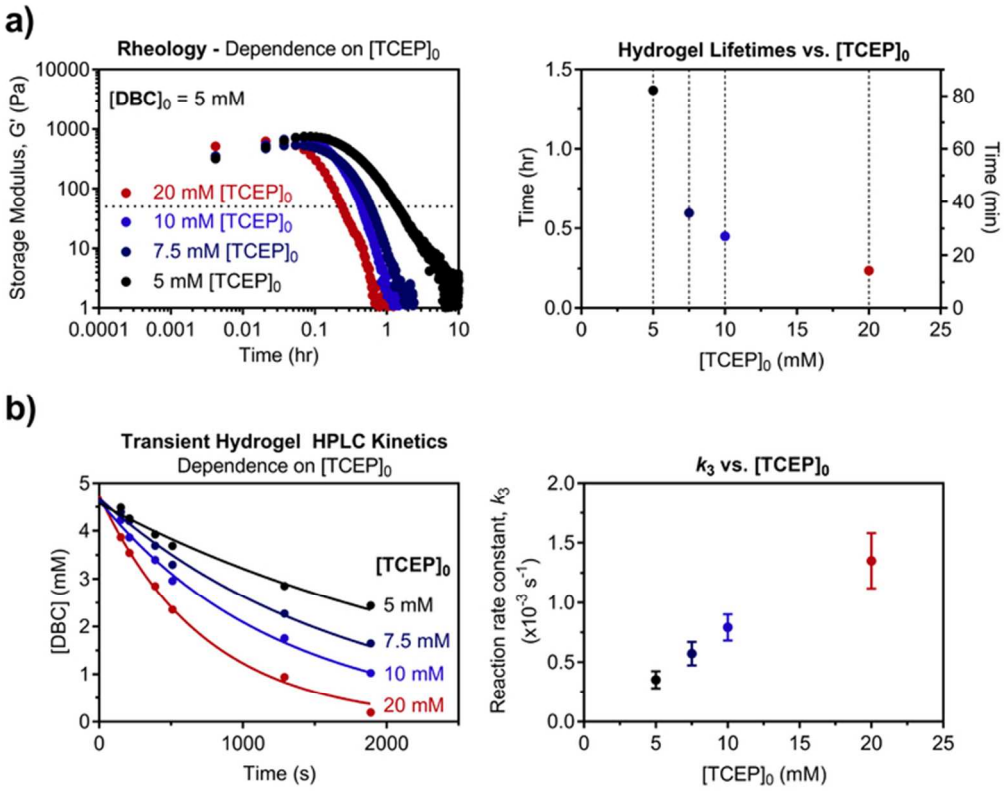

Figure 3. a) Time-resolved rheology of 5 mM **DBC** hydrogels shows a decrease in the hydrogel lifetimes with increasing concentrations of TCEP. b) Kinetic analysis of the rate of reduction of 5 mM **DBC** transient hydrogels by TCEP fits to a pseudo-first order kinetic equation. Error bars on uncertainty are the 95% confidence interval (*nlparci* function in *matlab*).

65x51mm (300 x 300 DPI)

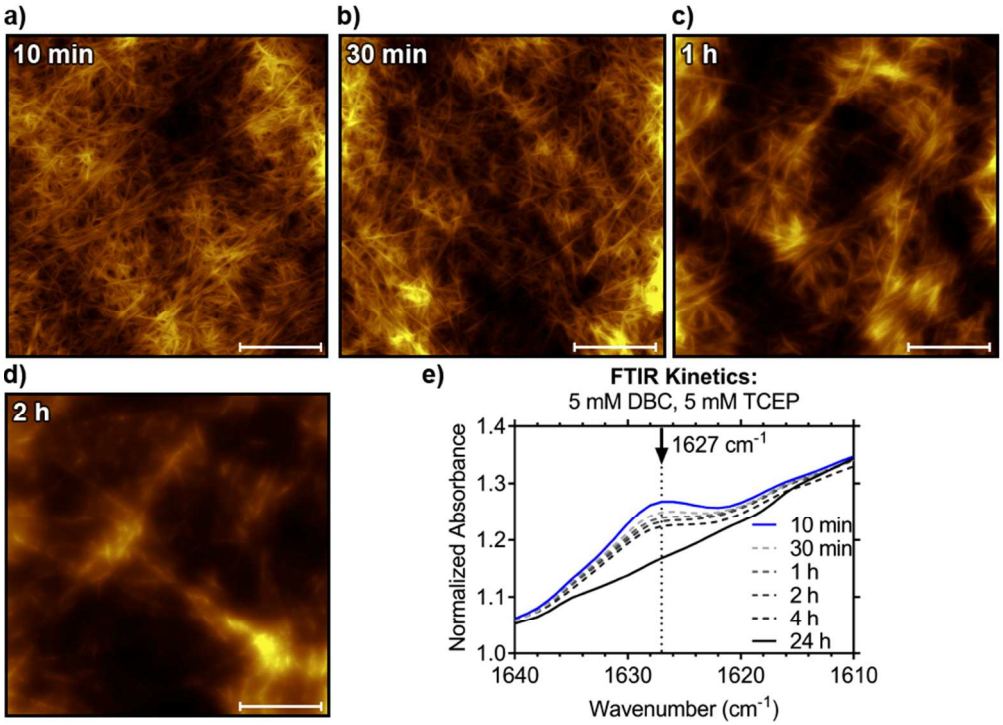

Figure 4. a-d) Time-resolved atomic force microscopy of a 5 mM **DBC** transient hydrogel with 5 mM TCEP; a) 10 min, b) 30 min, c) 1 h (60 min) and d) 2 h (120 min). e) Time-resolved FTIR on a 5 mM **DBC** transient hydrogel with 5 mM TCEP in D_2O shows a decrease in the amide C=O stretch at 1627 cm^{-1} with respect to time. Scale bars represent 1 μm.

82x59mm (300 x 300 DPI)

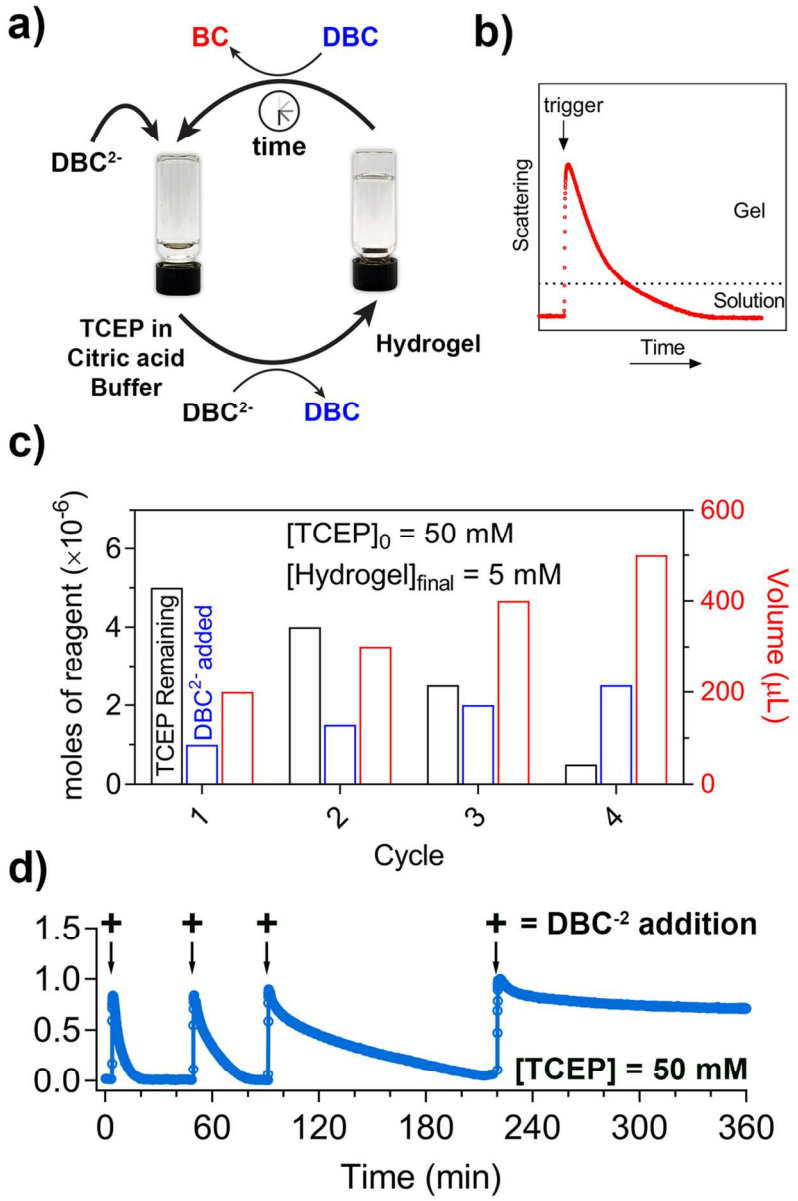

Figure 5. a) Schematic of the transient hydrogel cycles. The number of cycles can be programmed based on the starting concentration of TCEP. b) Typical time-resolved UV-vis scattering of the transient hydrogel cycle. c) Amount of TCEP remaining, **DBC^{2-}** added and volume change after each cycle for $[TCEP]_0$ = 50 mM. d) UV-vis scattering showing three transient hydrogel cycles with a starting concentration of TCEP = 50 mM.

96x144mm (300 x 300 DPI)